

A Duo of Graphene-Copper Based Wideband Planar Plasmonic Antenna Analysis for Lower Region of Terahertz (THz) Communications

Muhammad I. Khattak*, Muhammad Anab, and Nabeel Muqarrab

Abstract—In this article, a novel idea of designing a graphene based planar plasmonic patch antenna for terahertz wireless applications with detailed analysis is proposed. Based on the Surface Plasmon Polariton Waves (SPP) behaviour in graphene, a novel wideband planar graphene-based patch antenna is investigated here. As graphene with its wondered properties supports SPP in much lower infrared frequencies unlike the noble metals such as Gold and Nickle which support SPP at much higher frequencies, the proposed planar antenna works in THz gap (0.1–10 THz) by covering a range of frequencies from 0.1 THz and goes beyond 10 THz, thus covering the whole THz gap. The proposed antenna is a simple planar structure with overall size of $31.8 \times 6.4 \mu\text{m}^2$ having a Silicon with a relative permittivity (ϵ_r) of 11.9 used as a substrate material, and simple plane wave is used for excitation. Furthermore, radiating material comprises single layer graphene and copper with a partial ground of copper material, and for comparison purpose, only graphene layer as a radiating material is also analysed. Single layer graphene conductivity having chemical potential of 0.4 eV, relaxation time of 0.6 ps, and a temperature of 298 K is discussed. Parametric analysis for getting optimum results is also studied. The unity peak absorption of above 98% is observed throughout the resonating frequency range. The proposed design is numerically simulated in CST MWS v2020, and other parameters results, such as unity peak absorption and surface current, are also discussed.

1. INTRODUCTION

The past decade has witnessed that high-data-rate wireless communication systems have begun to share and use large amounts of information, thereby rapidly increasing the speed of data transmission. To transmit large amounts of information with high-speed data rates, current communication systems must require broadband and speeds of 10 to 100 Gbps as much as possible to meet ever-increasing speed requirements [1]. To meet the requirement for broadband and high-speed data transmission in high-speed communication systems, the frequency needs to be moved to a higher range. Therefore, electromagnetic spectrum researchers have observed a frequency range between the optical (infrared light) and microwave frequency regions, called near-infrared band or sub-millimeter wave, or THz frequency [2, 3]. The specific region of interest to the researchers is the frequency from 0.3 to 10 THz, called THz gap. THz radiation is also referred to by many other names in different branches of physics, including submillimetre radiation, THz waves, T-waves, T-light, T-rays, and T-Lux. THz gap exists with wavelength less than visible IR light but is greater than radio waves.

Like microwaves, THz radiation can penetrate and pass through a variety of materials, including clothing, paper, cardboard, wood, masonry, ceramics, and plastics with different attenuation levels [4].

Received 6 January 2021, Accepted 12 March 2021, Scheduled 22 March 2021

* Corresponding author: Muhammad Irfan Khattak (M.I.Khattak@uetpeshawar.edu.pk).

The authors are with the Microwave and Antenna Research Group, Electrical Engineering Department, UET Peshawar, Kohat Campus, Pakistan.

However, it cannot penetrate the liquids like water or metals, which means that the radiation of these frequencies has limited penetration through fogs or clouds. Additionally, compared to microwaves the penetration of these waves is not as deep. Many materials such as plastic explosives possess distinct fingerprints when spectroscopy of these materials is performed with THz radiations, so THz radiations can be used in security applications for weapon detections under fabrics. THz radiation can be used safely in medical imaging applications. The radiation coming from THz radiation is not harmful to body tissues (DNA) because it can only penetrate a few millimetres into the skin.

One of the many advantages of this particular frequency band is that due to the richness of the bandwidth, its data transmission rate is much higher than that of the current system [5]. Due to many unique features, such as wide impedance bandwidth, compact device size (up to nanometers), high speed, and very high resolution, the terahertz band can be used in many fields, including agriculture [6], wireless on-chip Network (WNoC) [7], medical and bioindustry [8], metal characterization [9], spectroscopy, imaging, high-resolution radar communication, and the recent new generation of high-speed wireless communication systems [10–13]. Because of its low photon energy and harmlessness to human tissues, THz imaging is safe, less invasive than x-ray, and good to use for medical purposes. It penetrates several millimetres in tissues with some reflection. Furthermore, THz radiation is used to detect epithelial cancer cells. This process is painless, safe, and noninvasive. The airport security is another application where THz radiations can play their role in metal detections as these radiations can pass through fabrics and plastics but not the metals. For example, due to the high spatial density THz, hidden weapons can now be easily detected, as well as fingerprints left by many materials at THz frequency, which is convenient for the detection of drug and explosive substances. Other imaging applications include cavity inspection and drug curing inspection.

For any application we need to understand the basic concepts of THz antennas, which are the method used to transmit and receive THz radiation. The antenna functions as a transmitter when a voltage is applied, whereby the excited carriers from the film/conducting material are transmitted via an optical pulse resulting in an electromagnetic pulse. As a receiver, the antenna works when a current amplifier is applied to the contact. As opposed to voltage which is used for transmitter, when the time-dependent field hits the antenna, it creates a measurable unique current proportional to the original source. The quality of radiation depends largely on the material and the shape of the antenna. For example, metallic antennas have a low radiation efficiency in THz radiation. This is often problematic for THz signals. The quality of THz signals in THz radiation often affects the applications in which the system can be useful.

Despite that, THz regime amongst the current challenges is one, confronting electronic and photonic material and device engineering [14]. Moreover, the propagation of THz wave over long distance with micro-wavelength is limited because it suffers from high signal attenuation because of the atmospheric molecular absorption due to which researchers are of the view that THz frequency cannot be considered as a broadcasting frequency, but rather it can be used for point-to-point and indoor communications. Therefore, the development of high-efficiency antennas, high-performance modulators and detectors operating in the terahertz band, and new technologies that can improve the performance of terahertz wireless communication will make terahertz communication a reality in the next few years.

For this reason, recently, methods of manufacturing nano-scale and micro-scale devices and effective methods of finding effective conductive materials to develop THz devices have been actively studied. Conventional metal antennas are used independently of microelectronics in conventional wireless communication systems. By simply reducing the size, conventional metal antennas on the order of a few microns cannot be simply used for communication devices that work in the THz frequency range [15], because the physical characteristics of the device will change dramatically, and at higher frequencies there are various limitations at the nanoscale, with the most prominent being the low mobility of charge carriers in the nanoscale metal-based structure. So, it would result in high attenuation and less efficient nano-scale system (low efficiency) as the traditional metallic antennas are highly lossy at the THz resonant frequency primarily due to the low mobility of electrons [16]. The solution to these challenges and lossy behaviour is the exploration of metamaterial based nano-structures and characteristics of new materials and new devices at high frequencies [17].

Graphene, a 2-D material which is successfully exfoliated in 2004 [18], has attracted huge interest in the implementation of new devices at THz frequencies due to its numerous wonder properties. One

atomic thick, graphene made up of carbon atoms arranged in a hexagonal lattice manner making a honeycomb like crystalline structure, possesses unique numerous characteristics like chemical, thermal, mechanical, electronic, and optical properties has been potentially investigated in numerous application extending from ultra-high speed nano transistor up to transparent solar cells, surface plasmon polariton in graphene, and meta-materials [19–22]. Thus, using graphene as a conducting material instead of ordinary metals could be a possible solution to the above-mentioned challenges and problems. Several approaches have been devised so far for the fabrication of single or multilayer graphene like chemical oxidation of graphite [23, 24], Chemical Vapour Deposition (CVD) [25–31], mechanical cleavage [32], atmospheric pressure graphitization of Silicon Carbide (SiC) [33], and epitaxy growth in ultra-high vacuum [34].

Graphene has gained much interest in last decade in academic and industry fields to scaled-down circuits and antennas to micro and nano levels by implementing it in integrated circuits and chipsets. Graphene based terahertz plasmonic antennas working in THz band not in visible and infrared regions are proposed as an attractive solution for the ongoing nano wireless technologies [35, 36].

Graphene supports Surface Plasmon Polariton (SPP) which is the core phenomenon used in plasmonic nano-antennas, nano-filters, etc., because of the complex surface conductivity $\sigma_g(\omega, \mu_c, \tau, T)$ of graphene which plays an important role in SPP. Being a function of multi-parameters, graphene complex surface conductivity can be tuned, so a tuneable resonance frequency design can be achieved, by simply varying any of the parameters like radian frequency (ω), chemical potential μ_c (μ_c by itself depends on chemical doping, carrier density and electrostatic gate bias), relaxation time (τ), and temperature (T). Electromagnetic wave (EM) properties like propagation, polarization, and radiation can be modified by virtue of graphene sheet with tuning the conductivity of graphene mainly by chemical doping or electrostatic gate bias [37].

Confined EM waves when being coupled to surface electric charges at the boundary between the noble metals, like gold or silver and dielectric material, result in surface plasmon polariton waves at the interface. Graphene also supports SPP waves in THz and mid-infrared regions like the noble metals, but due to the complex surface conductivity of graphene, the key differences among the characteristics of graphene and noble metals are more confinement, low losses, tuneable complex conductivity, and mechanical strength. Noble metals are normally used as a radiating element in plasmonic devices at near infrared and visible frequency regions (up to several hundreds of THz), because noble metals have large negative real and small imaginary parts of dielectric permittivity at above mentioned frequency regions [38]. Wireless communication systems at infrared and visible regions have some serious drawbacks like non-line of sight communication being not possible, atmospheric absorption, low range, etc. Due to intrinsic properties like tuneable surface conductivity, high mobility carriers, etc., graphene supports the propagation of SPP waves but at much lower frequencies up to three order lower than noble metals, i.e., in the range of 0.1 up to a few THz. SPP waves are excited at the boundary between graphene layer and dielectric substrate [36–38].

Initially graphene was used as a parasitic layer in metallic antenna in order to improve the radiation characteristics of antenna, and thus it opens a door for graphene to be used in antenna applications [39]. Then in 2011, the idea of Transverse Magnetic Surface Plasmon Polariton Waves (TM SPP) were conceived on a single layer graphene sheet [40–42]. Due to the intrinsic property of slow propagation of SPPs in graphene, small-scale, and low-profile, graphene can be actively used as a radiating material in graphene antennas [42]. As a result, in recent few years numbers of research ideas have been published in order to demonstrate the radiation characteristics of graphene [39, 43–45]. Formerly, various graphene based plasmonic patch antenna configurations have been considered an interesting and challenging subject of research [46–50]. Due to its minimal power consumption, small size of few microns, and improved antenna characteristics, graphene-based antennas are favourable for rigorous constraint wireless communications and applications. Normally, graphene-based antennas are composed of either single layer or a few layers of graphene as a radiating material impinged on a metallic ground with a dielectric substrate in between them.

In this research article, a novel idea of designing a graphene based planar plasmonic patch antenna for THz wireless applications is analysed and investigated in details. The proposed antenna possesses a simple planar structure, working on THz gap (0.1–10 THz) by covering a range of frequencies from 0.1 THz and going beyond 10 THz, thus covering the whole THz gap. The overall size of antenna is

$31.8 \times 6.4 \mu\text{m}^2$ having a Silicon with a relative permittivity (ϵ_r) of 11.9 used as a substrate material, and simple plane wave is used for excitation. Furthermore, radiating material comprises the combination of single layer graphene and copper with a partial ground of copper material being used. For comparison purpose, the overall graphene as a radiating material is also used. Single layer graphene conductivity having chemical potential of 0.4 eV, relaxation time of 0.6 ps, and a temperature of 298 K is also discussed along with the parametric analysis for getting optimum results. The proposed designed is numerically simulated in CST MWS v2020. In Section 2, graphene conductivity modelling is discussed. In Section 3, dispersion equation is studied, while in Section 4, simulated results and antenna design are discussed. In Section 5, the article is concluded.

2. GRAPHENE CONDUCTIVITY MODELLING

The complex surface conductivity of graphene mainly comprises two parts according to the Kubo formula: intra-band $\sigma_{\text{intra-band}}$, which is mainly due to the electron-hole pair generation and recombination phenomena and inter-band $\sigma_{\text{inter-band}}$, which actually correspond to free carriers conductivity [51, 52]. When the frequency range is below the infrared, i.e., THz range, the effect of intra-band contribution dominates; otherwise, inter-band contribution is predominant [51]. It is hypothesized that there exists no external magnetic field, so the graphene conductivity is isotropic having both intra-band and inter-band terms [53], as shown in Equation (1).

$$\sigma_g(\omega, \mu_c, \tau, T) = \sigma_{\text{intra-band}} + \sigma_{\text{inter-band}} \quad (1)$$

where the intra-band term in graphene conductivity of Eq. (1) can be calculated as

$$\sigma_{\text{intra-band}} = \frac{ie^2 K_B T}{\pi \hbar^2 (\omega + 2i\Gamma)} \left[\frac{\mu_c}{K_B T} + 2 \ln \left(e^{\frac{\mu_c}{K_B T}} + 1 \right) \right] \quad (2)$$

The inter-band term in graphene conductivity of Eq. (1) can be approximated for $K_B T \ll |\mu_c| \hbar \omega$ as

$$\sigma_{\text{inter-band}} = \frac{ie^2}{4\pi \hbar} \ln \left[\frac{2|\mu_c| - (\omega + 2i\Gamma) \hbar}{2|\mu_c| + (\omega + 2i\Gamma) \hbar} \right] \quad (3)$$

where K_B denotes the Boltzmann's constant; $\hbar = h/2\pi$ represents the reduced Planck constant; and $\Gamma = 1/2\tau$ is the scattering rate.

The tangential electric field \mathbf{E} product complex surface conductivity of graphene $\sigma_g(\omega, \mu_c, \tau, T)$ defines the surface current density \mathbf{J} on graphene sheet as mentioned below

$$\hat{n} \times (|H|_{x=0^+} - |H|_{x=0^-}) = J_{\text{surf}} = \sigma_g(\omega, \mu_c, \tau, T) \times E \quad (4)$$

The edge effect of the graphene sheet on its surface conductivity having lateral size greater than 100 nm can be ignored [54, 55].

Real and imaginary parts of the single layer graphene conductivity having chemical potential of 0.4 eV, relaxation time of 0.6 ps, and a temperature of 298 K are depicted in Figure 1. Clearly, a decline behaviour can be observed in the real and imaginary parts of the graphene surface conductivity with the increase in frequency. Apparently, higher surface conductivity occurs because chemical potential (0.4 eV) can finally lead to lower losses, hence high efficiency can be accomplished.

3. DISPERSION EQUATION FOR SURFACE PLASMON POLARITON

Propagation properties of SPP wave in graphene sheet can be determined by the complex propagation constant k_{SPP} which can be defined as $k_{\text{SPP}} = k_o(n_{\text{eff}})$, where k_o represents the free space wave number, and n_{eff} denotes the complex effective index of SPP modes. Permittivity and permeability of the materials surrounding the graphene sheet have a great effect on k_{SPP} .

Both Transverse Magnetic (TM) and Transverse Electric (TE) SPP modes are supported by graphene. Nevertheless, due to the imaginary part of the complex conductivity of graphene, TM SPP mode can be propagated in THz frequency range. Complex propagation constant k_{SPP} of TM mode can be determined from the following dispersion equation of SPP [56];

$$\sqrt{n^2 - n_{\text{eff}}^2} + n^2 \sqrt{n^2 - n_{\text{eff}}^2} + \frac{4\pi}{c} \sigma_\omega \sqrt{1 - n_{\text{eff}}^2} \sqrt{n^2 - n_{\text{eff}}^2} = 0 \quad (5)$$

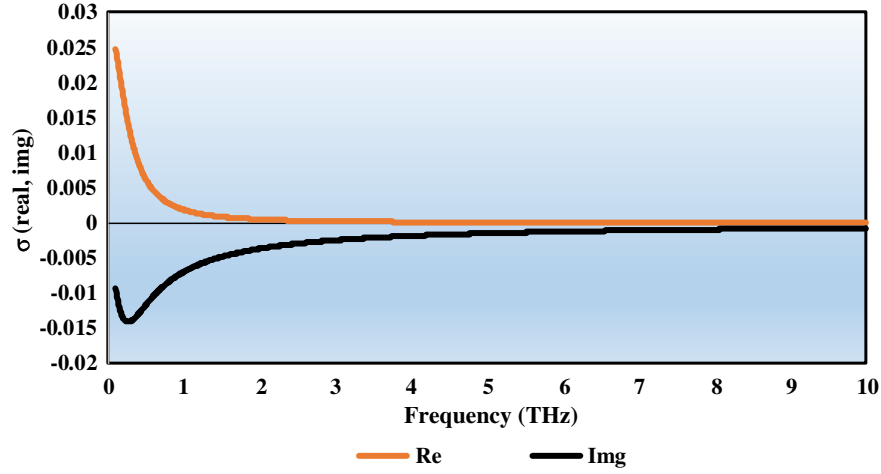


Figure 1. Real and imaginary parts of complex surface conductivity.

where n represents the refractive index of dielectric material used as a substrate, and σ_ω denotes the conductance of the graphene layer.

Dispersion equation of TM SPP mode can also be determined using alternative approach as given below [57]

$$\frac{\epsilon_{r1}}{\sqrt{k_{\text{SPP}}^2 - (\epsilon_{r1}\omega^2/c_0^2)}} + \frac{\epsilon_{r2}}{\sqrt{k_{\text{SPP}}^2 - (\epsilon_{r2}\omega^2/c_0^2)}} = -i \frac{\sigma_\omega}{\omega\epsilon_0} \quad (6)$$

It should be noted that graphene layers greatly affect the designed circuits. Single layer graphene is more practical for THz circuits, such as THz transmission line and filters, than multilayer graphene. However, multilayer graphene is used for efficiency improvement.

4. ANTENNA DESIGN

The novelty of the proposed design is kept in its simple planar structure, comprising a radiating patch which is a combination of graphene-copper layers, substrate material, and a copper partial ground. The proposed antenna design is based upon the effect of increasing patch sizes from down to bottom and vice versa. Furthermore, this effect introduces the concept of varying the impedances, along with generation extra edges, as in graphene radiation of plasmons occurs from the edges of the radiating surface. Similarly, the induction of copper patches in the proposed design reduces the electrons speed as in graphene the electron mobility is 1000,000 greater than copper, and this effect induces a form of capacitor with slower charging rate, copper being one of its plates. The front, exploded, perspective, and back views of the proposed structure are shown in Figures 2(a), (b), (c), and (d). The overall size ($L_s \times W_s$) of the proposed antenna is $31.8 \times 6.4 \mu\text{m}^2$ having a Silicon with a relative permittivity (ϵ_r) of 11.9 used as a substrate material. The final design is achieved by varying the impedance of radiating patch from top to bottom in order to achieve the targeted wide THz band. Dimensions of the left half radiating patch are shown in the exploded view in Figure 2(b), whereas the right half radiating patch is the inverted version of left half radiating patch having a difference of copper only in its two segments. There exists a slot of size $0.2 \times 1.2 \mu\text{m}^2$. Single layer graphene having a thickness of 0.345 nm with characteristics of 0.4 eV chemical potential, 0.6 ps relaxation time, and 298 K temperature is used. The thickness of copper is the same as that of graphene whereas the thickness of substrate (H_s) is $0.745 \mu\text{m}$. The dimensions of the partial ground ($L_g \times W_g$) is $5 \times 6.4 \mu\text{m}^2$.

Simple plane wave having direction in negative z -axis is used for excitation with a simulation setup of Perfect Electric Conductor (PEC) and a Perfect Magnetic Conductor (PMC) boundaries conditions along x and y -axes, respectively. Design parameters are listed in Table 1.

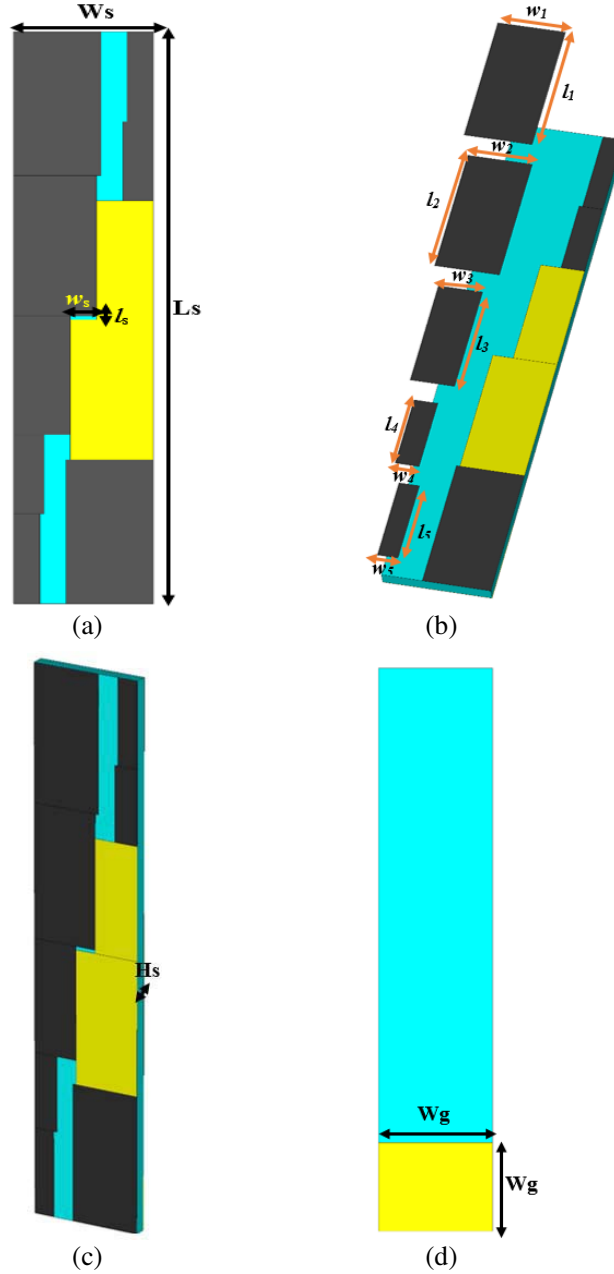


Figure 2. (a) Front, (b) exploded, (c) perspective, and (d) back views of the graphene based planar plasmonic patch (PPP) antenna.

5. RESULTS ANALYSIS

Along with its simple planar structure the proposed design also operates over a wide range of frequencies covering almost all the THz gap (0.1–10 THz). Simulated reflection coefficient (S_{11} (dB)) of the investigated design is depicted in Figure 3. The investigated design operates over a frequency range started from 0.1 THz up to 10 THz with a deep curve at 0.59 THz having S_{11} of -48.4 dB. In Figure 3, simulated S_{11} (dB) of only graphene layer as a patch is also compared with the proposed design having graphene-copper combined radiating patch. There is a slight variation in S_{11} (dB) of only graphene layer as a patch towards left side, which clearly supports SPP wave propagation theory for graphene.

The tunability effect of graphene complex conductivity, which is the intrinsic property of the

Table 1. Parameters list of proposed graphene based PPP antenna.

Parameters	Values (μm)						
L_s	31.8	W_s	6.4	L_g	5	W_g	6.4
l_1	8	w_1	4	l_2	7.8	w_2	3.8
l_3	6.6	w_3	2.6	l_4	4.4	w_4	1.4
l_5	5	w_5	1.2	l_s	0.2	w_s	1.2

graphene conductivity due to the chemical potential parameter as can be verified from Equations (2) & (3), is also studied for two different chemical potential values. By changing chemical potential from 0.4 eV (proposed) to 1 eV, tunability effect is illustrated in Figure 4, both for graphene only and graphene-copper combination. Clearly, it can be seen from Figure 4 that the results are improved by 10–15% for chemical potential 1 eV, and we can easily improve/increase the bandwidth on upper side, i.e., beyond 10 THz if needed. However, the only limitation for higher value of chemical potential is that practically high gate voltage will be required for getting high value of chemical potential.

In order to get the optimum design parameters for the proposed antenna, parametric analysis is

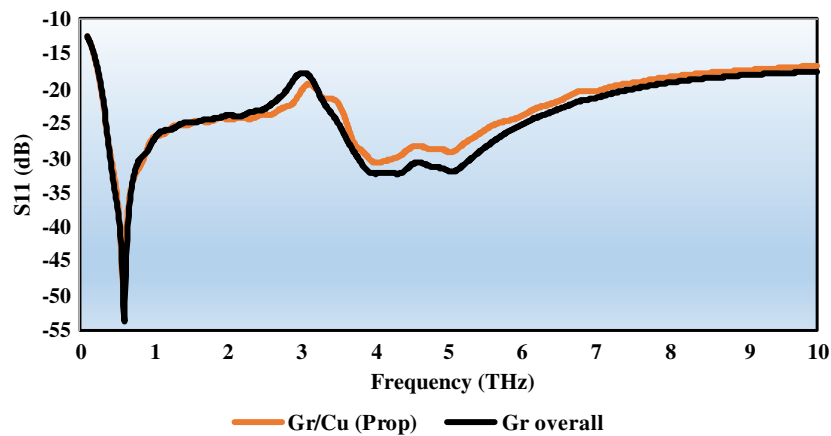


Figure 3. Comparison of simulated S_{11} of Gr overall & Gr-Cu combined patch of proposed graphene based PPP antenna.

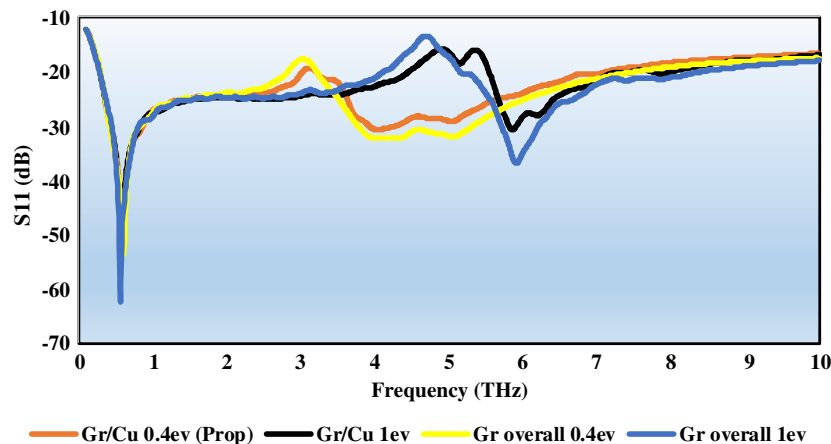


Figure 4. Effect of chemical potential on proposed graphene based PPP antenna.

performed. Effects on the performance of designed antenna by parameters of the proposed design, like width of substrate (W_s), size of ground plane, and length of substrate (L_s), are also investigated here. Variation in impedance bandwidth and return loss of the proposed graphene-based PPP antenna with respect to the length and width of substrate and ground plane are summarized in Figures 5(a), (b),

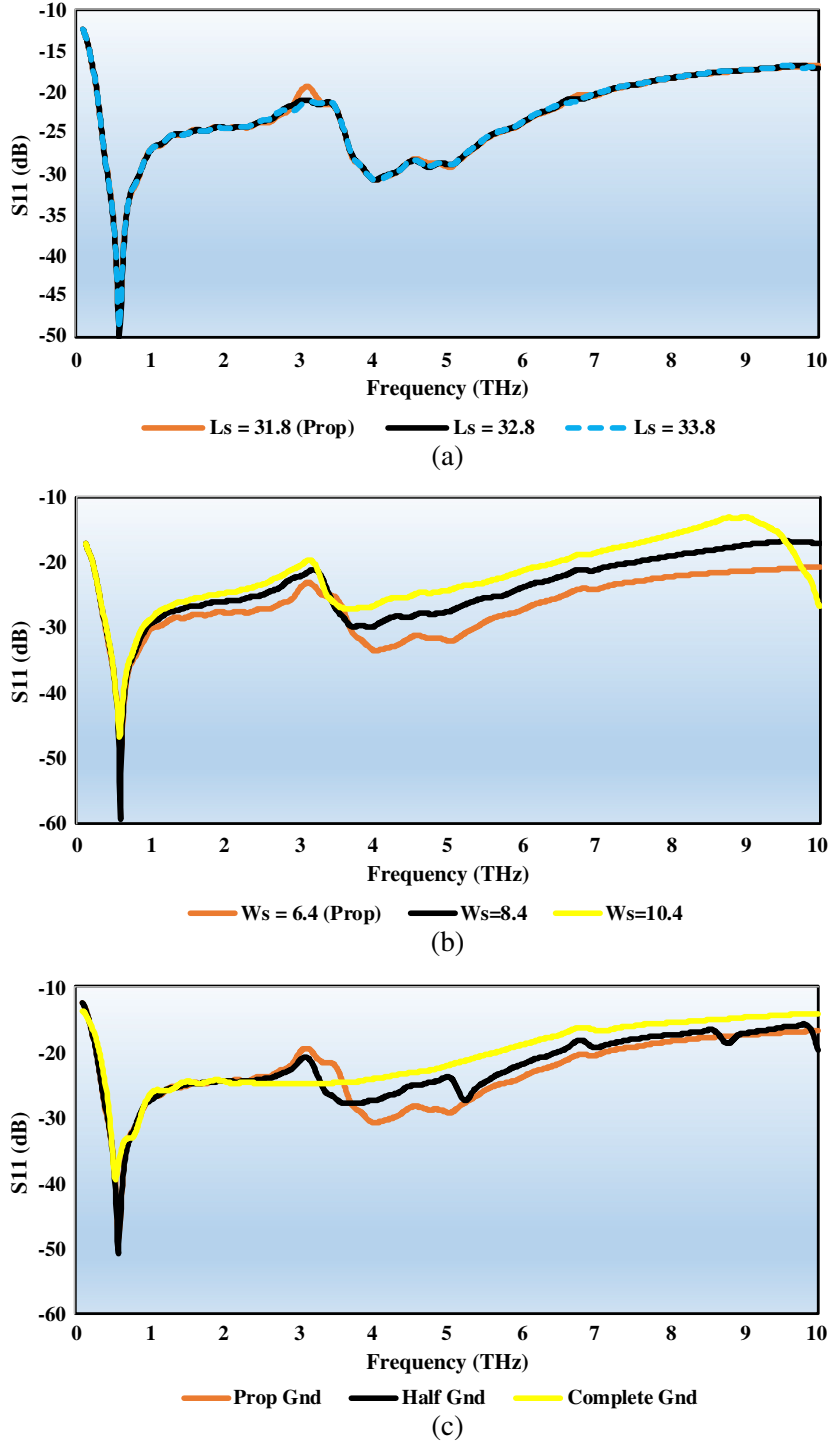


Figure 5. Variation in impedance bandwidth and return loss of proposed graphene-based PPP antenna w.r.t, (a) length of substrate, (b) width of substrate and (c) ground plane.

& (c).

With increasing length of substrate (L_s), almost negligible effect on the performance of proposed design is observed as illustrated in Figure 5(a). However, the width of substrate (W_s) has a significant effect on the impedance bandwidth of the proposed antenna, i.e., with increasing width of substrate, impedance bandwidth and return loss get reduced with only a slight increase in deep curve (return loss) at a frequency 0.59 THz at W_s equal to $8.4 \mu\text{m}$, as shown in Figure 5(b). Finally, the effect of ground plane on the investigated design is also studied, i.e., by increasing the size of ground plane, impedance bandwidth also gets reduced, and a decrease in return loss is observed as shown in Figure 5(c). Ultimately, partial ground is proposed in order to achieve a wide impedance bandwidth.

Input impedance is the property of an antenna, with whose help a clear understanding of how well the proposed antenna matches the incident source can be made. Figure 6 depicts the real and imaginary parts of the input impedance of the investigated antenna over the entire frequency operating range. The orange line illustrated in Figure 6 signifies the real part of the input impedance, while the black line signifies the imaginary part of the input impedance. A good agreement between the input impedance spectra and a return loss can be justified from Figure 6, which is in accordance with the matching condition.

Figure 7 depicts the dramatic absorption of the proposed graphene-based planar plasmonic patch antenna under the normal excitation being illuminated by plane wave with normal incidence to antenna

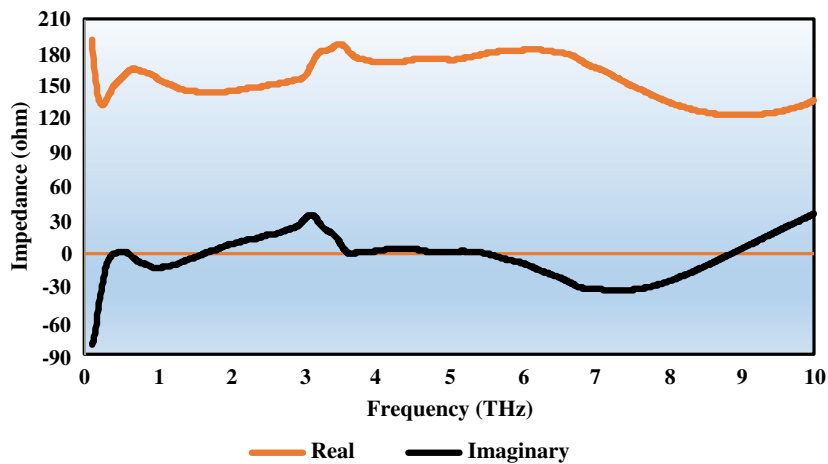


Figure 6. Real & imaginary part of the input impedance of proposed graphene-based PPP antenna.

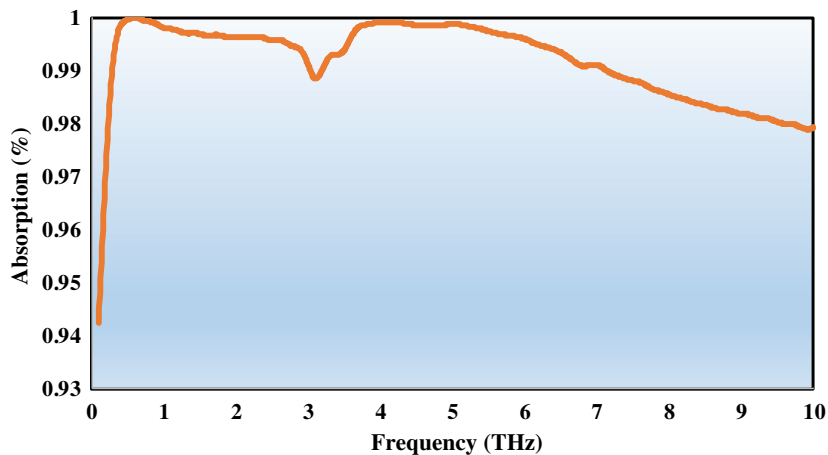


Figure 7. Absorption spectra of the proposed graphene based PPP antenna.

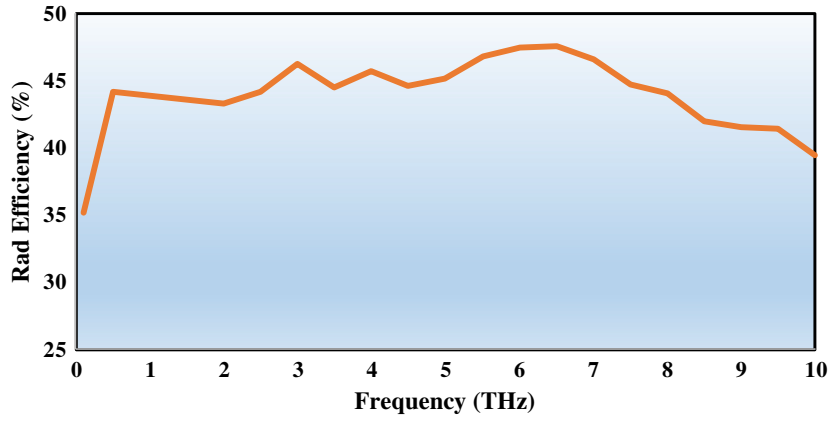


Figure 8. Radiation efficiency of the proposed graphene based PPP antenna.

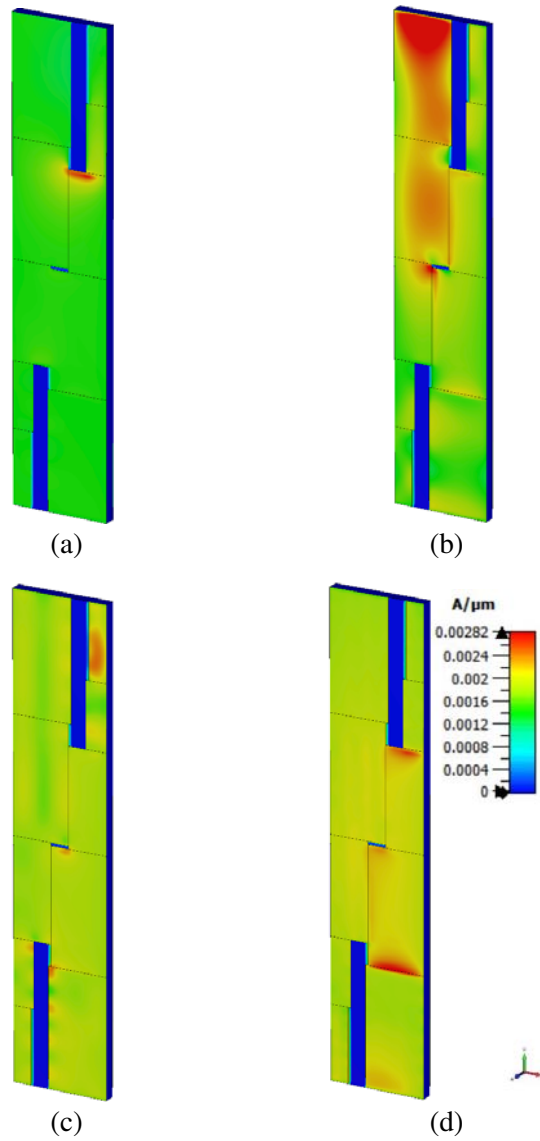


Figure 9. Surface current distribution of proposed graphene based PPP antenna at (a) 0.59 THz, (b) 3 THz, (c) 5 THz and (d) 7 THz.

surface. The unity peak absorption of above 98% can be observed throughout the resonating frequencies range.

Additionally, radiation efficiency analysis of the proposed graphene-based PPP antenna is analysed since efficiency is the core factor of the graphene antennas. Figure 8, depicts the radiation efficiency of the proposed antenna. Radiation efficiency of the proposed antenna is above 40%, and a maximum efficiency of almost 48% can be verified from Figure 8. Surface current distributions at four different operating frequencies, i.e., 0.59, 3, 5, and 7 THz are shown in Figures 9(a), (b), (c), & (d). Furthermore, the intensity of current is maximum at the edges of the radiating surface.

6. CONCLUSIONS

In conclusion, based on the Surface Plasmon Polariton Waves (SPP) behaviour in graphene, a novel and efficient wideband graphene-based planar plasmonic patch antenna for THz wireless applications has been investigated. As graphene supports SPP in much lower infrared frequencies, noble metals such as gold and Nickel support SPP at much higher frequencies. Accordingly, the investigated planar antenna works in THz gap (0.1–10 THz) by covering a range of frequencies from 0.1 THz and going beyond 10 THz, thus covering the whole THz gap. The novelty of the designed antenna is its simple planar structure operating over a wide range of frequency with radiating material comprising single layer graphene and copper with a partial ground of copper material. Complex surface conductivity of the proposed single layer graphene having chemical potential of 0.4 eV, relaxation time of 0.6 ps, and a temperature of 298 K is also studied. Finally, parametric analysis is performed to get optimum results for tunability effect, unity peak absorption of above 98% throughout the resonating frequencies range, and other parameters such as surface current distribution, radiation efficiency, and input impedance.

REFERENCES

1. Koenig, S., D. Lopez-Diaz, J. Antes, F. Boes, R. Henneberger, A. Leuther, A. Tessmann, R. Schmogrow, D. Hillerkuss, R. Palmer, and T. Zwick, "Wireless sub-THz communication system with high data rate," *Nature Photonics*, Vol. 7, No. 12, 977–981, 2013.
2. Liu, D., U. Pfeiffer, J. Grzyb, and B. Gaucher, *Advanced Millimeter-wave Technologies: Antennas, Packaging and Circuits*, John Wiley & Sons, 2009.
3. Grischkowsky, D., S. Keiding, M. van Exter, and C. Fattinger, "Far-infrared time-domain spectroscopy with terahertz beams of dielectrics and semiconductors," *JOSA B*, Vol. 7, No. 10, 2006–2015, 1990.
4. Kazemi, A. H. and A. Mokhtari, "Graphene-based patch antenna tunable in the three atmospheric windows," *Optik*, Vol. 142, 475–482, 2017.
5. Sadeghzadeh, R. A. and F. B. Zarrabi, "Metamaterial Fabry-Perot cavity implementation for gain and bandwidth enhancement of THz dipole antenna," *Optik*, Vol. 127, No. 13, 5181–5185, 2016.
6. Li, B., Y. Long, H. Liu, and C. Zhao, "Research progress on Terahertz technology and its application in agriculture," *Transactions of the Chinese Society of Agricultural Engineering*, Vol. 34, No. 2, 1–9, 2018.
7. Deb, S., A. Ganguly, P. P. Pande, B. Belzer, and D. Heo, "Wireless NoC as interconnection backbone for multicore chips: Promises and challenges," *IEEE Journal on Emerging and Selected Topics in Circuits and Systems*, Vol. 2, No. 2, 228–239, 2012.
8. Nishizawa, J. I., T. Sasaki, K. Suto, T. Yamada, T. Tanabe, T. Tanno, T. Sawai, and Y. Miura, "THz imaging of nucleobases and cancerous tissue using a GaP THz-wave generator," *Optics Communications*, Vol. 244, Nos. 1–6, 469–474, 2005.
9. Naftaly, M., A. P. Foulds, R. E. Miles, and A. G. Davies, "Terahertz transmission spectroscopy of nonpolar materials and relationship with composition and properties," *International Journal of Infrared and Millimeter Waves*, Vol. 26, No. 1, 55–64, 2005.
10. Sirisha, M. and M. Arun, "Dual-band reconfigurable graphene-based patch antenna in terahertz band for wireless network-on-chip applications," *IET Micr., A. & Prop.*, Vol. 11, 2104–2108, 2017.

11. Seyedsharbaty, M. M. and R. A. Sadeghzadeh, "Antenna gain enhancement by using metamaterial radome at THz band with reconfigurable characteristics based on graphene load," *Optical and Quantum Electronics*, Vol. 49, No. 6, 221, 2017.
12. McIntosh, A. I., B. Yang, S. M. Goldup, M. Watkinson, and R. S. Donnan, "Terahertz spectroscopy: A powerful new tool for the chemical sciences," *Chemical Society Reviews*, Vol. 41, No. 6, 2072–2082, 2012.
13. Chernomyrdin, N. V., M. E. Frolov, S. P. Lebedev, I. V. Reshetov, I. E. Spektor, V. L. Tolstoguzov, V. E. Karasik, A. M. Khorokhorov, K. I. Koshelev, A. O. Schadko, and S. O. Yurchenko, "Wide-aperture aspherical lens for high-resolution terahertz imaging," *Review of Scientific Instruments*, Vol. 88, No. 1, 014703, 2017.
14. Dhillon, S. S., M. S. Vitiello, E. H. Linfield, A. G. Davies, M. C. Hoffmann, J. Booske, C. Paoloni, M. Gensch, P. Weightman, G. P. Williams, and E. Castro-Camus, "The 2017 terahertz science and technology roadmap," *Journal of Physics D: Applied Physics*, Vol. 50, No. 4, 043001, 2017.
15. Kleine-Ostmann, T. and T. Nagatsuma, "A review on terahertz communications research," *Journal of Infrared, Millimeter, and Terahertz Waves*, Vol. 32, No. 2, 143–171, 2011.
16. Pourahmadazar, J. and T. A. Denidni, "Millimeter-wave planar antenna on flexible polyethylene terephthalate substrate with water base silver nanoparticles conductive ink," *Microwave and Optical Technology Letters*, Vol. 60, No. 4, 887–891, 2018.
17. Chen, H. T., W. J. Padilla, J. M. Zide, A. C. Gossard, A. J. Taylor, and R. D. Averitt, "Active terahertz metamaterial devices," *Nature*, Vol. 444, No. 7119, 597–600, 2006.
18. Novoselov, K. S., A. K. Geim, S. V. Morozov, D. Jiang, Y. Zhang, S. V. Dubonos, I. V. Grigorieva, and A. A. Firsov, "Electric field effect in atomically thin carbon films," *Science*, Vol. 306, No. 5696, 666–669, 2004.
19. Wang, X., L. Zhi, and K. Müllen, "Transparent, conductive graphene electrodes for dye-sensitized solar cells," *Nano Letters*, Vol. 8, No. 1, 323–327, 2008.
20. Geim, A. K. and K. S. Novoselov, "The rise of graphene," *Nature Materials*, Vol. 6, 183–191, 2007.
21. Vakil, A. and N. Engheta, "Transformation optics using graphene," *Science*, Vol. 332, No. 6035, 1291–1294, 2011.
22. Jablan, M., H. Buljan, and M. Soljačić, "Plasmonics in graphene at infrared frequencies," *Physical Review B*, Vol. 80, No. 24, 245435, 2009.
23. Stankovich, S., D. A. Dikin, R. D. Piner, K. A. Kohlhaas, A. Kleinhammes, Y. Jia, Y. Wu, S. T. Nguyen, and R. S. Ruoff, "Synthesis of graphene-based nanosheets via chemical reduction of exfoliated graphite oxide," *Carbon*, Vol. 45, No. 7, 1558–1565, 2007.
24. Tung, V. C., M. J. Allen, Y. Yang, and R. B. Kaner, "High-throughput solution processing of large-scale graphene," *Nature Nanotechnology*, Vol. 4, No. 1, 25, 2009.
25. Emtsev, K. V., A. Bostwick, K. Horn, J. Jobst, G. L. Kellogg, L. Ley, J. L. McChesney, T. Ohta, S. A. Reshanov, J. Röhrhl, and E. Rotenberg, "Towards wafer-size graphene layers by atmospheric pressure graphitization of silicon carbide," *Nature Materials*, Vol. 8, No. 3, 203–207, 2009.
26. Berger, C., Z. Song, T. Li, X. Li, A. Y. Ogbazghi, R. Feng, Z. Dai, A. N. Marchenkov, E. H. Conrad, P. N. First, and W. A. De Heer, "Ultrathin epitaxial graphite: 2D electron gas properties and a route toward graphene-based nanoelectronics," *The Journal of Physical Chemistry B*, Vol. 108, No. 52, 19912–19916, 2004.
27. Novoselov, K. S., A. K. Geim, S. V. Morozov, D. Jiang, Y. Zhang, S. V. Dubonos, I. V. Grigorieva, and A. A. Firsov, "Electric field effect in atomically thin carbon films," *Science*, Vol. 306, No. 5696, 666–669, 2004.
28. Kim, K. S., Y. Zhao, H. Jang, S. Y. Lee, J. M. Kim, K. S. Kim, J. H. Ahn, P. Kim, J. Y. Choi, and B. H. Hong, "Large-scale pattern growth of graphene films for stretchable transparent electrodes," *Nature*, Vol. 457, No. 7230, 706–710, 2009.
29. Obraztsov, A. N., E. A. Obraztsova, A. V. Tyurnina, and A. A. Zolotukhin, "Chemical vapor deposition of thin graphite films of nanometer thickness," *Carbon*, Vol. 45, No. 10, 2017–2021, 2007.

30. Reina, A., X. Jia, J. Ho, D. Nezich, H. Son, V. Bulovic, M. S. Dresselhaus, and J. Kong, "Large area, few-layer graphene films on arbitrary substrates by chemical vapor deposition," *Nano Letters*, Vol. 9, No. 1, 30–35, 2009.
31. Chae, S. J., F. Güneş, K. K. Kim, E. S. Kim, G. H. Han, S. M. Kim, H. J. Shin, S. M. Yoon, J. Y. Choi, M. H. Park, and C. W. Yang, "Synthesis of large-area graphene layers on poly-nickel substrate by chemical vapor deposition: Wrinkle formation," *Advanced Materials*, Vol. 21, No. 22, 2328–2333, 2009.
32. Li, X., W. Cai, J. An, S. Kim, J. Nah, D. Yang, R. Piner, A. Velamakanni, I. Jung, E. Tutuc, and S. K. Banerjee, "Large-area synthesis of high-quality and uniform graphene films on copper foils," *Science*, Vol. 324, No. 5932, 1312–1314, 2009.
33. Reina, A., S. Thiele, X. Jia, S. Bhaviripudi, M. S. Dresselhaus, J. A. Schaefer, and J. Kong, "Growth of large-area single- and bi-layer graphene by controlled carbon precipitation on polycrystalline Ni surfaces," *Nano Research*, Vol. 2, No. 6, 509–516, 2009.
34. De Parga, A. V., F. Calleja, B. M. C. G. Borca, M. C. G. Passeggi, Jr., J. J. Hinarejos, F. Guinea, and R. Miranda, "Periodically rippled graphene: Growth and spatially resolved electronic structure," *Physical Review Letters*, Vol. 100, No. 5, 056807, 2008.
35. Abadal, S., E. Alarcón, A. Cabellos-Aparicio, M. C. Lemme, and M. Nemirovsky, "Graphene-enabled wireless communication for massive multicore architectures," *IEEE Communications Magazine*, Vol. 51, No. 11, 137–143, 2013.
36. Akyildiz, I. F., J. M. Jornet, and C. Han, "TeraNets: Ultra-broadband communication networks in the terahertz band," *IEEE Wireless Communications*, Vol. 21, No. 4, 130–135, 2014.
37. Hanson, G. W., "Dyadic Green's functions and guided surface waves for a surface conductivity model of graphene," *Journal of Applied Physics*, Vol. 103, No. 6, 064302, 2008.
38. Hosseininejad, S. E., N. Komjani, and M. T. Noghani, "A comparison of graphene and noble metals as conductors for plasmonic one-dimensional waveguides," *IEEE Transactions on Nanotechnology*, Vol. 14, No. 5, 829–836, 2015.
39. Dragoman, M., A. A. Muller, D. Dragoman, F. Coccetti, and A. R. Plana, "Terahertz antenna based on graphene," *Journal of Applied Physics*, Vol. 107, No. 10, 104313, 2010.
40. Vakil, A. and N. Engheta, "Transformation optics using graphene," *Science*, Vol. 332, No. 6035, 1291–1294, 2011.
41. Jablan, M., H. Buljan, and M. Soljačić, "Plasmonics in graphene at infrared frequencies," *Physical Review B*, Vol. 80, No. 24, 245435, 2009.
42. Llatser, I., C. Kremers, A. Cabellos-Aparicio, J. M. Jornet, E. Alarcón, and D. N. Chigrin, "Graphene-based nano-patch antenna for terahertz radiation," *Photonics and Nanostructures — Fundamentals and Applications*, Vol. 10, No. 4, 353–358, 2012.
43. Tamagnone, M., J. S. Gomez-Diaz, J. R. Mosig, and J. Perruisseau-Carrier, "Reconfigurable terahertz plasmonic antenna concept using a graphene stack," *Applied Physics Letters*, Vol. 101, No. 21, 214102, 2012.
44. Wang, X. C., W. S. Zhao, J. Hu, and W. Y. Yin, "Reconfigurable terahertz leaky-wave antenna using graphene-based high-impedance surface," *IEEE Transactions on Nanotechnology*, Vol. 14, No. 1, 62–69, 2014.
45. Llatser, I., C. Kremers, and D. N. Chigrin, "Radiation characteristics of tunable graphenes in the terahertz band," *6th European Conference on Antennas and Propagation (EUCAP)*, 194–198, 2011.
46. Amanatiadis, S. A. and N. V. Kantartzis, "Design and analysis of a gate-tunable graphene-based nanoantenna," *2013 7th European Conference on Antennas and Propagation (EuCAP)*, 4038–4041, 2013.
47. Thampy, A. S., M. S. Darak, and S. K. Dhamodharan, "Analysis of graphene based optically transparent patch antenna for terahertz communications," *Physica E: Low-dimensional Systems and Nanostructures*, Vol. 66, 67–73, 2015.
48. Zhang, X., G. Auton, E. Hill, and Z. Hu, "Graphene THz ultra wideband CPW-fed monopole antenna," *1st IET Colloquium on Antennas, Wireless and Electromagnetics*, 1–16, IET, 2013.

49. Kempa, K., J. Rybczynski, Z. Huang, K. Gregorczyk, A. Vidan, B. Kimball, J. Carlson, G. Benham, Y. Wang, A. Herczynski, and Z. F. Ren, "Carbon nanotubes as optical antennae," *Advanced Materials*, Vol. 19, No. 3, 421–426, 2007.
50. Hanson, G. W., "Fundamental transmitting properties of carbon nanotube antennas," *IEEE Transactions on Antennas and Propagation*, Vol. 53, No. 11, 3426–3435, 2005.
51. Llatser Martí, I., C. Kremers, D. N. Chigrin, J. M. Jornet Montaña, M. C. Lemme, A. Cabellos Aparicio, and E. J. Alarcón Cot, "Radiation characteristics of tunable graphene antennas in the terahertz band," *Radioengineering*, Vol. 21, No. 4, 1–8, 2012.
52. Rouhi, N., S. Capdevila, D. Jain, K. Zand, Y. Y. Wang, E. Brown, L. Jofre, and P. Burke, "Terahertz graphene optics," *Nano Research*, Vol. 5, No. 10, 667–678, 2012.
53. Hanson, G. W., "Dyadic Green's functions and guided surface waves for a surface conductivity model of graphene," *Journal of Applied Physics*, Vol. 103, No. 6, 064302, 2008.
54. Cao, Y. S., L. J. Jiang, and A. E. Ruehli, "An equivalent circuit model for graphene-based terahertz antenna using the PEEC method," *IEEE Transactions on Antennas and Propagation*, Vol. 64, No. 4, 1385–1393, 2016.
55. Han, M. Y., B. Özyilmaz, Y. Zhang, and P. Kim, "Energy band-gap engineering of graphene nanoribbons," *Physical Review Letters*, Vol. 98, No. 20, 206805, 2007.
56. Dubinov, A. A., V. Y. Aleshkin, V. Mitin, T. Otsuji, and V. Ryzhii, "Terahertz surface plasmons in optically pumped graphene structures," *Journal of Physics: Condensed Matter*, Vol. 2, No. 14, 145302, 2011.
57. Jadidi, M. M., A. B. Sushkov, R. L. Myers-Ward, A. K. Boyd, K. M. Daniels, D. K. Gaskill, M. S. Fuhrer, H. D. Drew, and T. E. Murphy, "Tunable terahertz hybrid metal-graphene plasmons," *Nano Letters*, Vol. 15, No. 10, 7099–7104, 2015.